

ADVANCES IN FOREST FIRE RESEARCH

2022

Edited by

**DOMINGOS XAVIER VIEGAS
LUÍS MÁRIO RIBEIRO**

A study of fire and plume dynamics for static pool fires and their interaction with vegetation

Navya Muniraj; Weixuan Gong; Muthu Kumaran Selvaraj; Albert Simeoni*

Worcester Polytechnic Institute, Worcester, Massachusetts 01609, USA,
{nmuniraj, wgong, mselvaraj, asimeoni}@wpi.edu

**Corresponding author*

Keywords

Pool fire, Fire Plume, Vegetation, Prescribed burns

Abstract

Prescribed burns are an essential tool of fire management to reduce the impact and occurrence of wildfires. While managing prescribed burns, the smoke trajectory and downwind exposure to smoke are intimately coupled with the smoke production dynamics and the development of the fire plume in the vicinity of the fire front. In turn, the fire plume development is strongly coupled to fire behavior and the flow environment near the fire. This work aims at understanding fire behavior and plume development while interacting with vegetation at the large laboratory scale through experiments and modeling. In order to investigate these coupled processes, initially, flame and plume behavior from a static fire source was characterized. A rectangular pool fire fueled by diesel was used and point measurements of flow, temperature, and heat flux have been recorded. The mass burning rate was measured using a load cell. K-type thermocouples and bi-directional pressure probes have been used for measuring the velocity and temperature, respectively in the flame and plume zones. These data are used for validating a numerical model, the Fire Dynamics Simulator (FDS), for simulating pool fires and the model is subsequently used for predicting the plume interaction with vegetation. A Douglas fir tree, whose properties are well defined in literature, was used as vegetation. The Lagrangian particle model available in FDS was used to model the tree, which was represented with regular shape and size. It had foliage and different classes of wood split based on typical size (diameter) range. The bulk density of the tree was varied to replicate the systematic and controlled variation of the flow obstruction encountered by the plume and to provide realistic predictions of velocity, temperature, and heat flux within the vegetation. In the future, experiments with vegetation located in the plume region will be conducted to validate the numerical predictions.

1. Introduction

Prescribed burns are one of the commonly used fire management tools to reduce the impact and occurrence of wildfires. During prescribed burns, the fire and plume generated from the combustion of the surface fuel (such as pine needles) interacts with the raised vegetation. The fire and plume behavior are influenced by the non-burning raised vegetation through drag and heat transfer and they also have an impact on the raised vegetation when heating it. Similarly, the variability in vegetation also affects the flow, fire, and plume dynamics. In order to analyze such complex phenomena, the fire, which is the source of the plume, must be well characterized. Pool fires were chosen for study as they mimic the fire environment in prescribed burns and are relatively easy to control, while avoiding additional complexities due to fire spread. Generating a volume of smoke at the laboratory scale that is relevant to the field scale requires the use of medium and large-scale pool fires. Several works have been reported earlier on small scale pool fires (Prasad et al., 1999; Attar et al., 2013; Wu et al., 2020), which are typically less than 0.3 m in diameter. However, only limited research has been conducted on medium and large-scale pool fires (Wen et al., 2007; Sudheer et al., 2013; Xin et al., 2005; Wahlqvist et al., 2016; Stewart et al., 2021). These fires fall either in the transition or turbulent regime and are dominated by radiative heat transfer. Wen et al. (2007) conducted experimental and numerical study on medium-scale methanol pool fires. Temperature and velocity measurements were used to validate a numerical model available in FDS. (Sudheer et al., 2013) analyzed the temperature distribution and emissivity of gasoline pool fires with varying pool diameters (0.3 - 1 m). FDS was able to accurately predict the centerline temperature distribution and heat flux measurements for all the cases. Wahlqvist & van Hees (2016) used FDS to predict the mass loss rate of heptane pool fires with the inclusion of heat feedback from external sources, such as walls, and the oxygen concentration near the pool. Stewart et al. (2021) numerically investigated the ability of FDS to predict

medium and large-scale open pool fires of several hydrocarbon fuels including gasoline and diesel. Results showed that FDS predicted the three-step transient burning pattern of: fire growth, quasi-steady burning, and extinction, as observed in the experiments. However, for higher order hydrocarbon fuels such as diesel, when the pan is fully covered with flame, the model overpredicted the burning rate.

It is clear that there is a significant gap in reporting the flame characteristics and dynamics of medium and large-scale pool fires. The transient nature of the flame affects the plume dynamics, entrainment, and mass burning rate. Therefore, it is essential to characterize the pool fires before investigating their interaction with vegetation. Furthermore, the interaction of vegetation with the plume and its impact on the fire environment have not been investigated yet. In this work, point measurements of flow, temperature, and heat flux at various locations in the plume and flame zones were carried out to validate a numerical model for predicting the dynamics of the flame and buoyant plume over a static pool fire. The validated model was then used with raised vegetation to analyze its influence on flow and plume dynamics relevant to a prescribed burn scenario.

2. Experimental methodology

A rectangular pan having a dimension of 68 cm × 63 cm × 6.3 cm was used to generate a diesel pool fire. Diesel flames are highly sooty, and it facilitates the visualization of plume during its interaction with the raised vegetation in the lab and field scale experiments. The rectangular shape has been chosen to allow creating larger fires in the future, by attaching multiple pans together. Figure 1 presents a schematic of the experimental setup. The pan was filled with 2 gallons (7.56 liters) of fuel to provide a steady burning time of 8 to 9 min. The pan was placed over a load cell with an accuracy of 0.1 g for measuring the mass loss rate of the burning fuel. K-type thermocouple with a bead diameter of 0.5 mm were used for measuring the temperature in the flame and plume zones. Velocity measurements were carried out using bi-directional pressure probe. Heat flux sensors (both convective and radiative) were used for measuring the convective and radiative heat flux from the flame. The center of the pool surface was taken as origin. The thermocouples and bi-directional pressure probes were located along the vertical direction (z-axis) 0.5 m from the pool surface and in arrays up to 3.5 m (see Fig. 1.a), while the heat flux sensors were located at 1, 2 and 3 m from the fuel surface and were offset by 1 m in the y-direction (not shown on Fig. 1.a). In the horizontal plane (x-axis), four arrays of thermocouples (a total of seven thermocouples spaced by 15 cm in each array) were fixed at heights of 1, 2, 3, and 3.5 m from the pool surface. Similarly, two bi-directional pressure probes were located on each horizontal plane (8 in total) spaced 15 cm apart from either side of the central probe. Since the boiling point of diesel quite high, a small amount (100 ml) of gasoline was added to the pool prior to ignition in order to facilitate the process. The pool ignited within two seconds when using a propane torch. Figure 1.b shows a flame photographed during the steady burning regime.

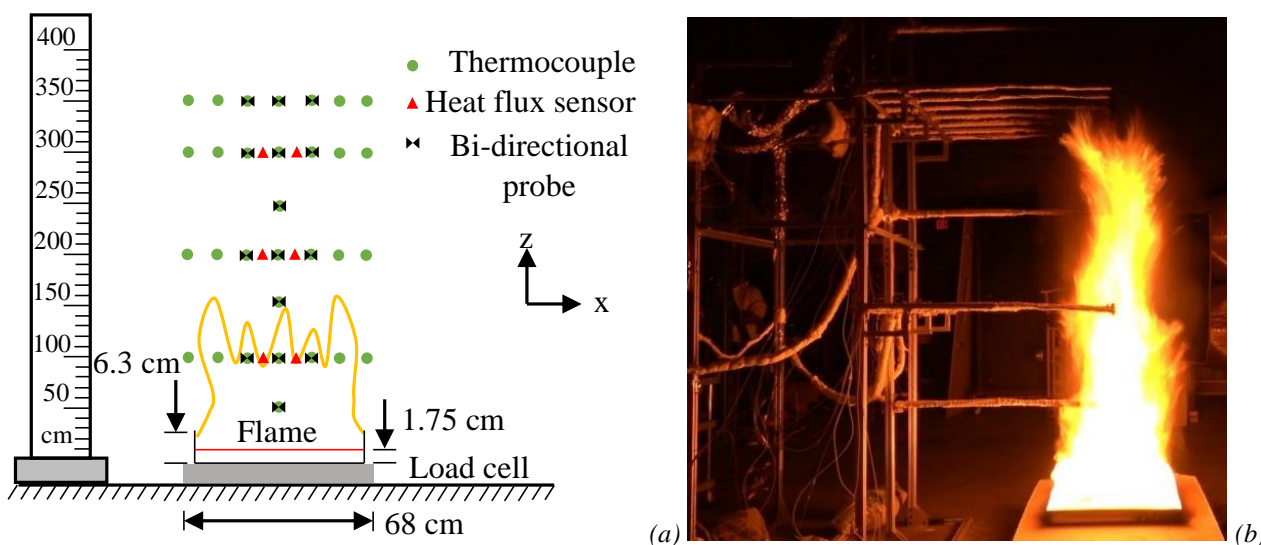


Figure 1- (a) Schematic of the experimental setup (b) flame photograph during steady state burning

3. Numerical approach

3.1. Computational domain

Numerical simulations were carried out using Fire Dynamics Simulator (FDS v6.7.7). Figure 2 shows a schematic of the computational domain used in the simulations. The dimensions of the domain were $6\text{ m} \times 6\text{ m} \times 8\text{ m}$. The bottom boundary was taken as an adiabatic wall. All other boundaries were open to atmosphere. In case of a reverse flow, ambient air ($\text{O}_2 - \text{N}_2$: 23.3% - 76.7%, by mass) at a temperature of 20°C entered the domain through the open boundaries. Dodecane, a surrogate of diesel was used as the fuel. The properties of diesel, adapted from Stewart et al., (2021) were used in the simulations. For simulations with vegetation (Fig. 2.b), the geometrical and thermo-physical properties of Douglas fir tree reported in Mell et al. (2009) were used. The domain was split into several multi-block meshes with uniform grid spacing in the z-direction (within each block). The total number of cells in the domain was around 2.8 million. Numerically, the pool was ignited by giving a constant heat flux of 300 kW/m^2 at the fuel surface to replicate the ignition time observed in the experiments. With this heat flux value, the pool ignited within 3 s.

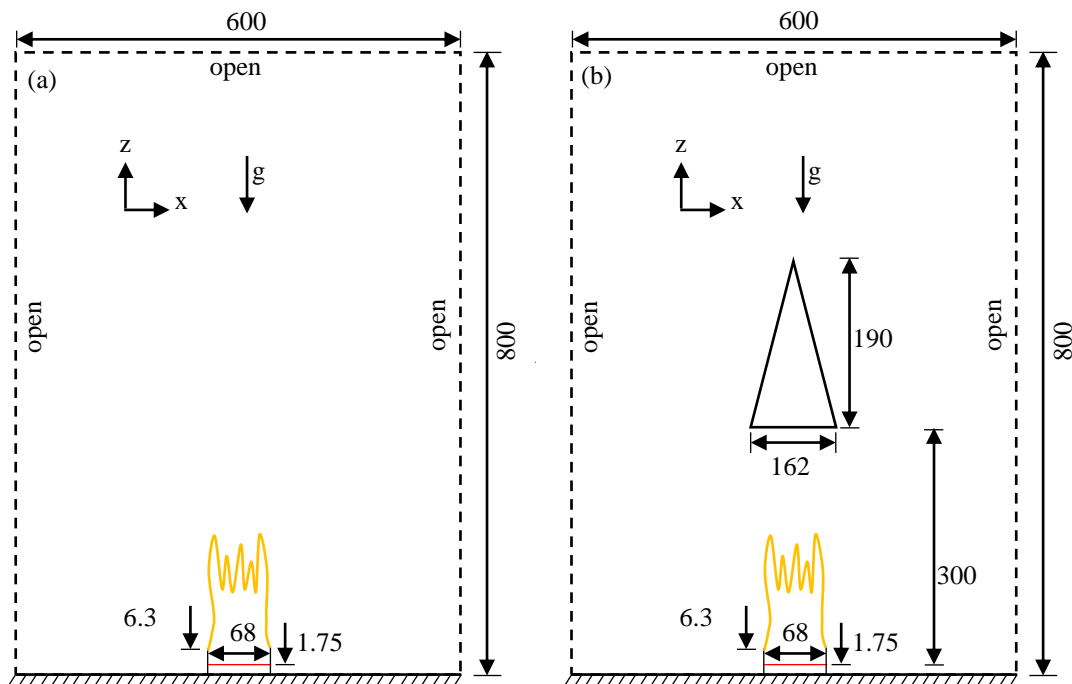


Figure 2- Schematic of the computational domain with (a) a diesel pool fire and (b) a Douglas fir tree located above the pool fire (the trunk was not represented) – Dimensions are in cm

4. Results and Discussion

Figure 3 presents the comparison of the predicted mass loss rate and temperature profiles with the experimental values, along the centerline at different heights above the fuel surface. In the experiments, first gasoline at the surface of the pool ignites and preheats the diesel pool to the boiling temperature. The flame height is low during this stage and the experimental mass burning rate (Fig. 3.a) gradually increases to an average steady state value of around 0.011 kg/s . It takes around 60 s to achieve steady state burning from the start of ignition ($t = 0\text{ s}$) and the average mass burning rate remains constant at 0.011 kg/s during the steady burning regime. It lasts from $t = 60\text{ s}$ to $t = 580\text{ s}$, for around 9 min. The burning rate then decreases and the flame extinguishes 2 min after the end of the steady burning regime.

In the simulations, the pool is ignited 3 s after ignition and the mass burning rate quickly reaches steady state (average around 0.0115 kg/s). Then, it slowly increases to 0.013 kg/s with a further increase in time (300 s). After $t=300\text{ s}$, the burning rate rapidly increases to 0.02 kg/s and then steeply decreases until flame extinction. The difference between the experimental and predicted mass burning rate is due to (1) the difference in the ignition process, (2) the difference in fuel properties used in the experiments and in the model (as reported in Stewart et al., 2021), (3) the neglect of internal convection within the pool in the model, while it can be quite

significant in this case because of the adiabatic boundary. The model underpredicts the temperature profiles at $z = 0.5$ m, however, the experimental trend is captured (see Fig. 3.b). The model accurately predicts the temperature in the flame zone ($z = 1$ m) and overpredicts it in the intermittent ($z = 1.5$ m), and plume zones ($z = 2.0$ and 3.5 m).

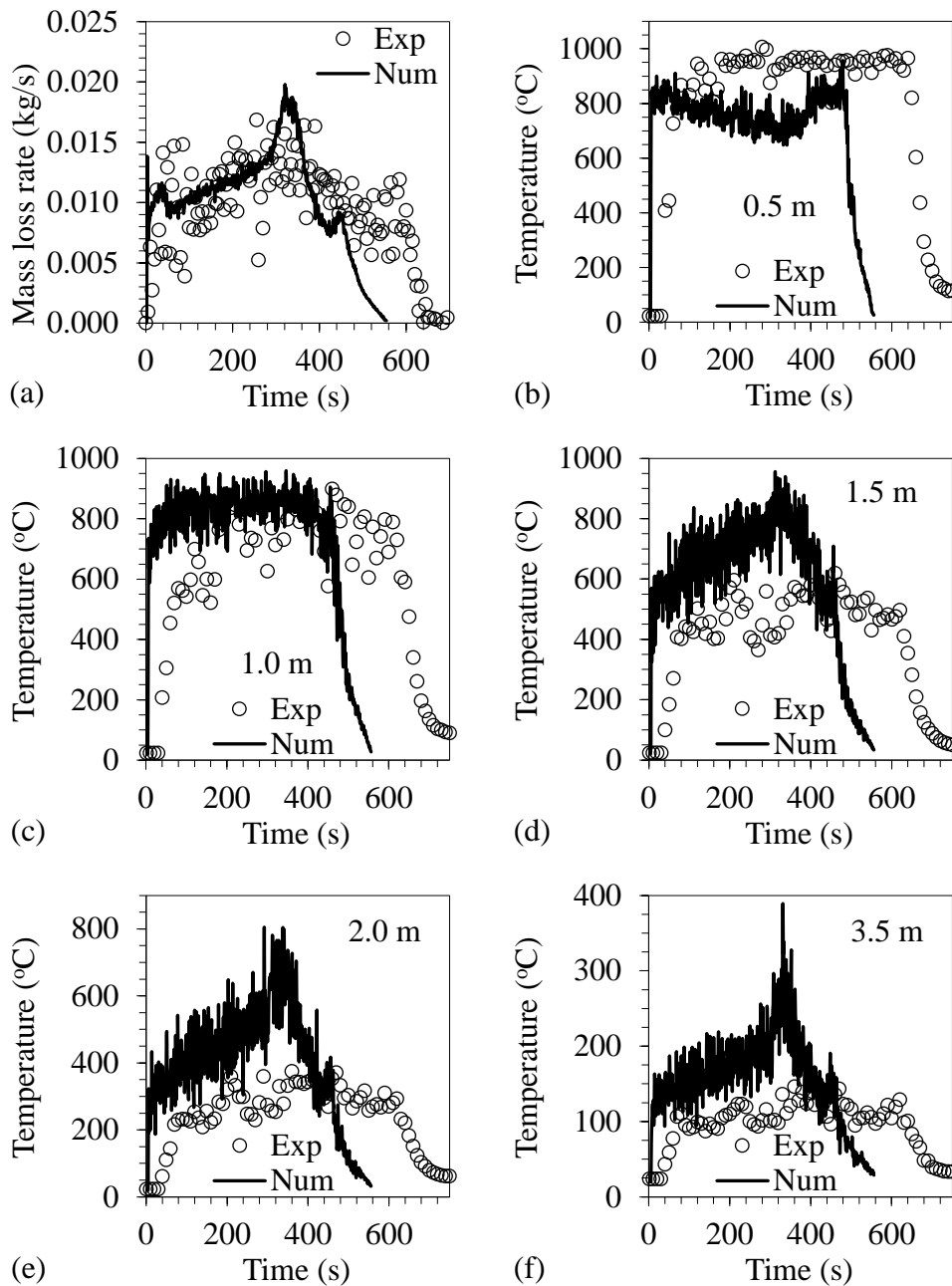


Figure 3- Comparison of predicted (a) mass loss rate and temperature profiles at (b) $z=0.5$ m, (c) $z=1.0$ m, (d) $z=1.5$ m, (e) $z=2.0$ m, (f) $z=3.5$ m to experimental data

Figures 4.a and 4.b show the comparison of temperature and water vapor mass fraction contours for cases with pool fire and pool fire with tree. The contours are plotted at 200 s after the start of simulation. The temperature in the flame zone is almost the same in both cases. However, there is a significant difference in the plume temperature above 2.5 m. For the case without tree, the plume temperature reduces to 100°C - 150°C above 4 m due to air entrainment and diffusion. On the other hand, for the case with tree, the temperature within the tree is around 250°C – 350°C. This results in moisture evaporation (and subsequent pyrolysis of vegetation) as indicated by higher values of water vapor mass fraction contours within the tree (0.02). Figures 4.c and 4.d show the velocity vectors and contours of dodecane and the oxygen mass fraction for these cases. The air entrainment and the acceleration of product gases due to buoyancy in the flame zone are clearly visible. In the vicinity of

the tree, a significant portion of the plume with sufficiently high velocity passes through the tree. Then, the flow velocity reduces due to drag by the fuel particles. Near the edge of the tree (base of the cone), a small portion of the plume is deflected away (as for a flow around an obstacle). However, the drag resulting from this behavior will strongly depend on the packing ratio inside the tree. The oxygen mass fraction within the tree is in the range of 0.16 - 0.23. The oxygen mixes with the pyrolysis gases but will not ignite the tree since the temperatures are not high enough. This justifies the distance chosen for locating the tree above the pool fire, which in this case is 3 m, as the objective of prescribed burns is to avoid burning or harming the trees.

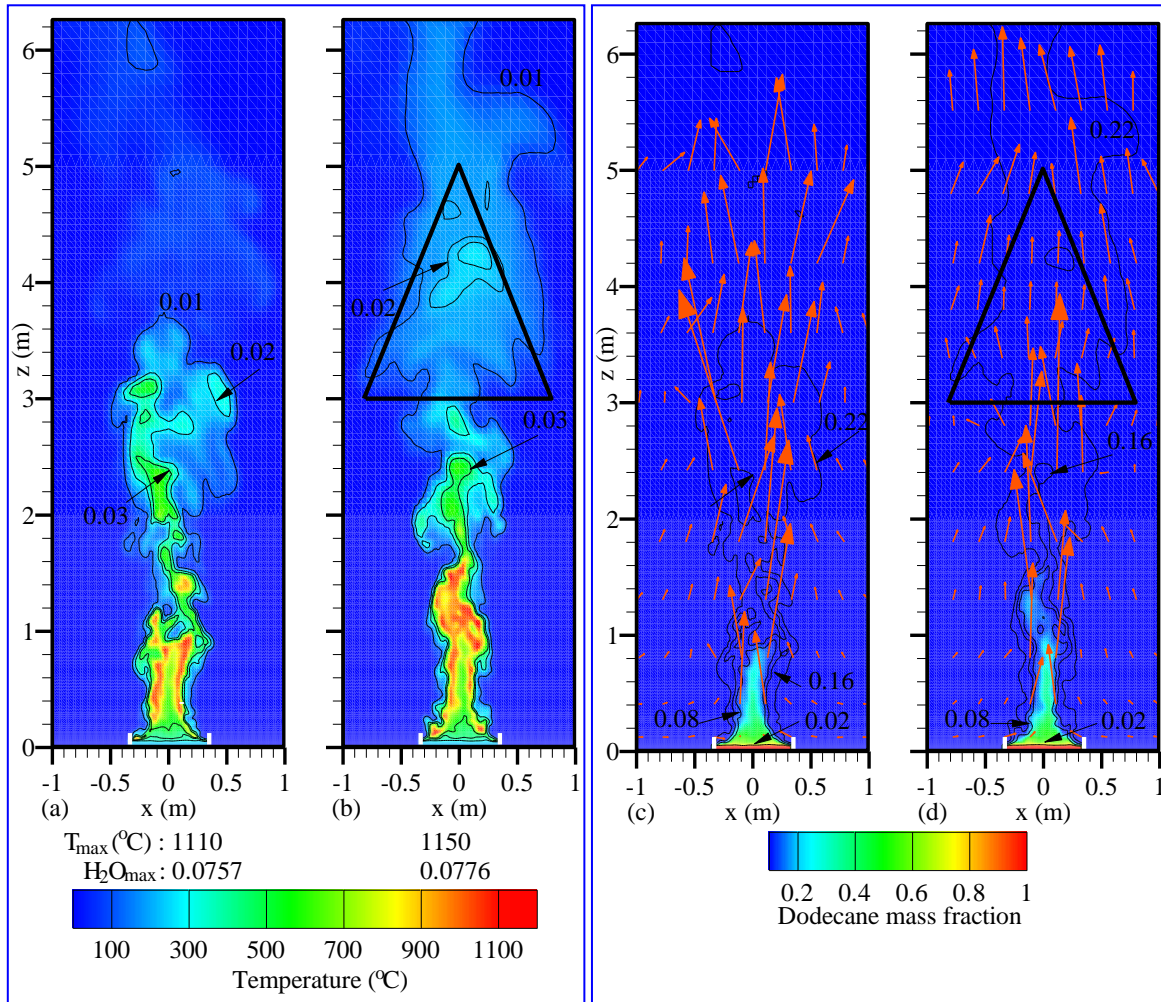


Figure 4 - (a), (b) Contours of temperature (colored) and water vapor mass fraction (lines) (c), (d) Contours of dodecane mass fraction (colored) and oxygen mass fraction (lines) with velocity vectors. The white lines represent the boundaries of the pan, and the triangle represents the Douglas fir tree.

5. Conclusions

An experimental and numerical study has been conducted as the first step of a larger study of the interaction between plume and vegetation during prescribed burns. The predicted mass burning rate and temperature were compared with measurements in a diesel pool fire. The model predicts a higher mass burning rate due to (1) the difference in ignition process, (2) the difference in fuel properties of diesel used in the experiments and that reported in the literature, which was subsequently used in the model, and (3) absence of sub-models to simulate convective heat transfer within the pool. The temperature is overpredicted in the intermittent and plume zones. Even though discrepancies exist, the model reveals some of the key processes such as moisture release within the vegetation which could be difficult to measure due to the presence of water vapor in the plume.

In the future, trees of various size and shape will be placed over the pool fire and point measurements of temperature, velocity, and heat flux will be recorded to model the drag and heat transfer within the vegetation. These sub-models will be included to validate and improve the accuracy of the numerical model.

6. Acknowledgement

The authors thank Abhinandan Singh for his help with the experiments.

7. References

- Attar, A.A., Pourmahdian, M., Anvaripour, B. (2013). Experimental Study and CFD Simulation of Pool Fires, *International Journal of computer applications*, 70(11), 9-15. 10.5120/12004-5790
- Fire Dynamics Simulator, User Guide, FDS v6.7.7. https://tsapps.nist.gov/publication/get_pdf.cfm?pub_id=913619
- Mell, W., Maranghides, A., McDermott, R., Manzello, S. (2009). Numerical simulation and experiments of burning Douglas fir trees. *Combustion and Flame*, 156, 2023-2041. <https://doi.org/10.1016/j.combustflame.2009.06.015>
- Prasad, K., Li, C., Kailasanath, K., Ndubizu, C., Ananth, R., Tatem, P.A. (1999). Numerical modelling of methanol pool fires, *Combustion Theory and Modelling*, 3, 743-768. <https://doi.org/10.1088/1364-7830/3/4/308>
- Stewart, J.R., Phylaktou, H.N., Andrews, G.E., Burns, A.D. (2021). Evaluation of CFD simulations of transient pool fire burning rates, *Journal of Loss Prevention in the Process Industries*, 71, 104495, <https://doi.org/10.1016/j.jlp.2021.104495>
- Sudheer, S., Saamil, D., Prabhu, S.V. (2013). Physical experiments and Fire Dynamics Simulator simulations on gasoline pool fires, *Journal of Fire Sciences*, 31(4), 309-329. <https://doi.org/10.1177/0734904112472953>
- Wahlqvist, J., van Hees, P. (2016). Implementation and validation of an environmental feedback pool fire model based on oxygen depletion and radiative feedback in FDS, *Fire Safety Journal*, 85, 35-40. <https://doi.org/10.1016/j.firesaf.2016.08.003>
- Wen, J.X., Kang, K., Donchev, T., Karwatzki, J.M. (2007). Validation of FDS for medium-scale pool fires, *Fire Safety Journal*, 42, 127-138. <https://doi.org/10.1016/j.firesaf.2006.08.007>
- Wu, B., Roy, S.P., Zhao, X. (2020). Detailed modeling of a small-scale turbulent pool fire, *Combustion and Flame*, 214, 224-237. DOI:10.1016/j.combustflame.2019.12.034
- Xin, Y., Gore, J.P., McGrattan, K.B., Rehm, R.G., Baum, H.R. (2005). Fire dynamics simulation of a turbulent buoyant flame using a mixture-fraction-based combustion model, *Combustion and Flame*, 141, 329-335. <https://doi.org/10.1016/j.combustflame.2004.07.001>